

Embedding Dependencies Within Distributionally Robust Optimization of Modern Power Systems

Adriano Arrigo, Jalal Kazempour, *Senior Member, IEEE*, Zacharie De Grève, *Member, IEEE*,
Jean-François Toubeau, *Member, IEEE*, and François Vallée, *Member, IEEE*

Abstract—The increasing share of renewables in the electrical energy generation mix comes along with an increasing uncertainty in power supply. In the recent years, distributionally robust optimization has gained significant interest due to its ability to make informed decisions under uncertainty, which are robust to misrepresentations of the distributional information (e.g., from probabilistic forecasts). This is achieved by introducing an ambiguity set that describes the uncertainty around an empirical distribution of all uncertain parameters. However, this set typically overlooks the inherent dependencies of uncertainty, e.g., space-time dependencies of renewable energy sources. This paper goes beyond the state of the art by embedding such dependencies within the definition of the ambiguity set. In particular, we propose a metric-based ambiguity set with an additional constraint on dependence structure, using copula theory. We develop a conic reformulation which is kept generic such that it can be applied to any decision-making problem under uncertainty in power systems. As an example, we illustrate the performance of our proposed distributionally robust model applied to an energy and reserve dispatch problem in a power system with a high share of renewables.

Index Terms—Distributionally robust optimization, copula, space-time dependencies, energy and reserve dispatch.

Notation: \mathbb{R} and \mathbb{R}^+ represent the set of all real and non-negative real numbers, respectively. The cardinality of a set is written within vertical bars $|\cdot|$. We use vector notation, and $(\cdot)^\top$ represents the transpose operator. The vector of ones is written $\mathbb{1}$, whose length is made clear from the context. When taking into account uncertainty, $\mathbb{E}^{\mathbb{Q}}[\cdot]$ represents the expectation operator with respect to distribution \mathbb{Q} . In addition, $\mathbb{Q}(\cdot)$ is the probability operator. We use tildes for random variables, e.g., $\tilde{\xi}$, and hats for observations of the random variable, e.g., $\hat{\xi}_i$. Observations are indexed by $i \in \{1, \dots, N\}$, where N is the number of observations, and may have a second subscript $k \in \{1, \dots, |\mathcal{W}|\}$ for insisting on the k^{th} dimension of the observation, e.g., ξ_{ki} . The symbol $\tilde{\xi} \sim \mathbb{Q}$ links the random variable to its distribution function, e.g., $\tilde{\xi} \sim \mathbb{Q}$.

I. INTRODUCTION

THE continuous balance between power injections and offtakes is paramount to ensure the safe operation of power systems, however it is being challenged by the uncertainty introduced by the weather-dependent renewable power

generation [1]. To cope with such an uncertainty, it is crucial to develop uncertainty-aware decision-making tools for operational and planning purposes. While the power system operators traditionally use a deterministic optimization approach by considering a single-point forecast of renewable power generation, stochastic approaches account for a probabilistic forecast, allowing to make more informed operational and planning decisions (depending on the forecast accuracy) [2].

The power system research community has put a lot of efforts in the last decades for developing various types of stochastic decision-making tools, ranging from scenario-based stochastic programming [3]-[4] to robust optimization [5]-[6] and chance-constrained programming [7]-[8]. Aiming to exploit the benefits of a recently developed approach that outperforms all previous techniques [9] and to fully leverage the information contained within a probabilistic forecast, we model the uncertainty using a Distributionally Robust Optimization (DRO) approach [10]-[11]. As our main contribution, we go beyond the current state of the art by developing a DRO approach for power systems that is aware of all potential dependencies (correlation) among uncertain parameters, in particular the space-time dependencies of renewable energy sources.

DRO allows to hedge against the inherent errors arising from modeling the probabilistic distribution that is typically derived from the probabilistic forecast. These errors may propagate to the resulting decisions and compromise the reliability and cost-efficiency of the power system. The exposure to uncertainty in the probability distribution itself is called *ambiguity* [12]. By design, DRO considers a family of potential distributions, the so-called ambiguity set, to hedge against any inexactness or biasedness of the distribution function¹. Owing to its appealing properties, one popular approach to define an ambiguity set is based on the Wasserstein probability metric², which calculates the distance between two distribution functions [15]. In the Wasserstein DRO approach, all distributions in the neighborhood of a central empirical distribution, based on historically observed samples of uncertainty, are collected and fed to the decision-making problem. Although this technique carefully handles the available information by

¹Unlike DRO that considers ambiguity, classical techniques such as scenario-based stochastic programming and robust optimization assume a perfectly known probability distribution.

²Another existing approach in the literature is moment-based ambiguity sets [13]-[14] which collect the distributions that share the same moments, e.g., mean and covariance. While this uncertainty modeling technique offers a tractable reformulation, it does not generally exploit the whole available empirical data to model uncertainty in an efficient way. In other words, the use of the whole empirical data is limited to the estimation of moments.

A. Arrigo, Z. De Grève, J.-F. Toubeau and F. Vallée are with the Power System and Market Research group, University of Mons, 31, Boulevard Dolez, 7000 Mons, Belgium. E-mails: {adriano.arrigo, zacharie.degrevé, jean-francois.toubeau, francois.vallee}@umons.ac.be

J. Kazempour is with the Department of Electrical Engineering, Technical University of Denmark, 2800 Kgs. Lyngby, Denmark. E-mail: seykaz@elektro.dtu.dk

TABLE I
RELEVANT FEATURES OF WORKS REPORTED IN THE LITERATURE AND THE
MODEL PROPOSED IN THIS PAPER

Reference	Peer-reviewed	Type of ambiguity set	Dependence structure	Type of dependence structure	Resulting model
[15], [25]	✓	Metric	✗	N.A. ¹	Conic
[19], [20]	✓	Moment-metric	✗	Linear	SDP ²
[21]	✗	Copula-based	✓	Non-linear with fixed marginals	Conic
[22], [26]	✓	Copula-based	✓	Non-linear with fixed marginals	Conic
[27]	✗	Copula-based	✓	Full non-linear	Conic
This paper	N.A.	Copula-based	✓	Full non-linear	Conic

¹ N.A.: Not applicable

² SDP: Semi-definite program

accounting for potential forecast errors, the ambiguity set may still contain erroneous distributions on which the optimal decision is made.

In the current literature, there is a willingness to enhance the Wasserstein ambiguity set by removing the unrealistic distributions of renewable power generation uncertainty. To do so, the supplementary constraints should be incorporated into the design of the ambiguity set. References [15] and [16] include the support information in the definition of Wasserstein ambiguity set, excluding distributions with unrealistic realizations of uncertainty. An example of such unrealistic distributions is those with a negative renewable power generation. References [17] and [18] include modality information, i.e., the number of spikes in a probability distribution, within the ambiguity set to get rid of unrealistic distributions, e.g., those with two or more spikes. References [19] and [20] embed information on dependencies, which is based on imposing the value of a covariance matrix in the ambiguity set definition. Overall, all these works allow to improve the representation of multi-dimensional uncertainties, however all have their own limitations and cannot represent the whole dependence structure.

Several additional works, as highlighted in Table I, have contributed towards embedding the full non-linear dependence information into the distributionally robust optimization. However, it is worth emphasizing that there are currently very few contributions in this research strand, especially focusing on power system applications. References [21]-[22] envisage the use of *copula* as the mathematical object to describe the full dependence structure among random variables. A copula is a distribution function with uniformly distributed marginals that contains solely information about the dependence structure among uncertain parameters [23]-[24]. To incorporate the dependence structure into the optimization problem, [21]-[22] introduce a constraint binding the Wasserstein distance between the copula of the distributions inside the ambiguity set and the one of the empirical distribution. In all these works, the marginals are fixed and assumed to be known. In other words, the only source of uncertainty stems from the dependence structure, and the ambiguity around the empirical distribution is no longer accounted for. This uncertainty scheme is usually suited for portfolio management problems in finance applications, but is expected to be insufficient for power system applications, where the marginal distributions of each renewable energy source are usually not available with high accuracy.

To address this issue, [27] represents, to the best of our knowledge, the first effort in the operations research literature

towards embedding the full dependence information along with the ambiguity around the empirical distribution function. To do so, the authors combine the findings in [21]-[22] with the classical approach to DRO [15]. They develop a Wasserstein ambiguity set that uses copula as the mathematical object to describe the full dependence structure among renewable energy sources.

In this paper, inspired by [27], we suggest a copula-based ambiguity set as the framework that *generalizes* (i) the constraint on the second-order moment, i.e., the one enforced in [19] and [20], and, (ii) the model with known marginals, i.e., the one used in [21]-[22] by enabling the DRO problem to consider *any* potential type of the correlation (not necessarily linear) among uncertain parameters. By this generalization, we are able to properly model the renewable power generation uncertainty that may exhibit any shape of dependencies [28]. To the best of our knowledge, this is the first effort in the literature to introduce copula-based ambiguity sets for power system applications. In particular, our contributions are threefold:

- (i) We first develop an optimization program in Lemma 1 which computes the value of an empirical cumulative distribution function. This allows us to link any distribution within the ambiguity set to its corresponding copula.
- (ii) Building up on Lemma 1, we develop a conic reformulation of a distributionally robust worst-case expectation problem³ in Theorem 1, using the proposed copula-based ambiguity set. Theorem 1 and the solution approach discussed in Appendix C are kept generic such that they could be applied to a broad range of problems in power systems.
- (iii) We apply the proposed conic formulation to a day-ahead distributionally robust energy and reserve dispatch problem with dependent renewable power generation uncertainty. We numerically show the benefits of the proposed reformulation compared to a state-of-the-art distributionally robust model, while identifying paths for future research.

The remainder of this paper is structured as follows. Section II provides a definition for the proposed copula-based ambiguity set to be used throughout the paper. Section III explains the reformulation process of a generic worst-case expectation problem under the copula-based ambiguity set. Section IV introduces the day-ahead distributionally robust energy and reserve problem and details the required reformulations. Section V discusses the proposed model through an extensive numerical analysis. Main conclusion and prospects are given in Section VI. Finally, the mathematical proofs of Lemma 1 and Theorem 1 are provided in Appendixes A and B, respectively, while the proposed solution approach for Theorem 1 is discussed in Appendix C.

³The worst-case expectation problem is a well-known problem in the field of DRO [29]. Its generic reformulation usually facilitates the application of DRO to any kind of problem where it naturally appears.

II. THE PROPOSED COPULA-BASED AMBIGUITY SET

A. Preliminaries

We start with the definition of an empirical distribution function. Consider N number of equiprobable historical observations of the uncertainty, i.e., $\hat{\xi}_i$, where $i = \{1, 2, \dots, N\}$. The empirical distribution $\hat{\mathbb{Q}}_N$ is defined as

$$\hat{\mathbb{Q}}_N = \frac{1}{N} \sum_{i=1}^N \delta_{\hat{\xi}_i}, \quad (1)$$

where $\delta_{\hat{\xi}_i}$ is the Dirac distribution centered on $\hat{\xi}_i$. Recall that every symbol with a hat, e.g., $\hat{\mathbb{Q}}_N$ and $\hat{\xi}_i$, corresponds to historical observations, and therefore, it is given.

Next, we define the Wasserstein probability metric. The metric $d_W(\mathbb{Q}, \hat{\mathbb{Q}}_N) : \mathcal{F} \times \mathcal{F} \rightarrow \mathbb{R}^+$ computes the distributional distance between two distribution functions \mathbb{Q} and $\hat{\mathbb{Q}}_N$ as the optimal value of a transportation problem between the probability mass of those two distributions [15]. The complete definition of this metric is given in the online appendix [30].

In the following, we define the well-known metric-based Wasserstein ambiguity set⁴, and eventually present our proposed copula-based ambiguity set.

B. Metric-Based Ambiguity Set \mathcal{M}_1

The metric-based ambiguity set \mathcal{M}_1 is defined as

$$\mathcal{M}_1 = \left\{ \mathbb{Q} \in \mathcal{F} \mid d_W(\mathbb{Q}, \hat{\mathbb{Q}}_N) \leq \theta_1 \right\}, \quad (2)$$

which contains a family of distributions \mathbb{Q} in the space of all distribution functions \mathcal{F} that are in the neighbourhood of the empirical distribution function $\hat{\mathbb{Q}}_N$. The distributional distance $d_W(\mathbb{Q}, \hat{\mathbb{Q}}_N)$ is limited to be lower than or equal to $\theta_1 \in \mathbb{R}^+$. This value is tuned by the decision-maker, and is referred to as the radius of the Wasserstein ambiguity set. One can intuitively interpret that a larger value of θ_1 yields an ambiguity set that contains more distributions, implying that the decision-maker is less certain about the true distribution of the underlying uncertainty.

C. Copula-Based Ambiguity Set \mathcal{M}_2

We first mathematically define copula \mathbb{C} of the distribution \mathbb{Q} . Let us consider $|\mathcal{W}|$ number of renewable power units, e.g., wind farms. Let $\tilde{\xi} \in \mathbb{R}^{|\mathcal{W}|} \sim \mathbb{Q}$. Unlike symbols with a hat that refer to historical observations, those with a tilde, e.g., $\tilde{\xi}$, correspond to uncertain parameters. The symbol $\tilde{\xi}_k$ refers to the uncertain generation of the renewable power unit k . Mathematically speaking, the copula \mathbb{C} of distribution \mathbb{Q} is defined as the cumulative distribution function of the uncertain parameter \tilde{U} [23]-[24], i.e.,

$$\begin{aligned} & (\tilde{U}_1, \dots, \tilde{U}_k, \dots, \tilde{U}_{|\mathcal{W}|}) \\ &= \left(F_1(\tilde{\xi}_1), \dots, F_k(\tilde{\xi}_k), \dots, F_{|\mathcal{W}|}(\tilde{\xi}_{|\mathcal{W}|}) \right), \quad (3) \end{aligned}$$

⁴The metric-based ambiguity set, given the Wasserstein probability metric, admits conic reformulations, which are popular in the field of DRO [31].

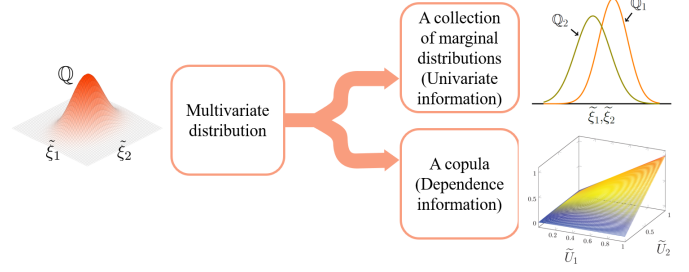


Fig. 1. Illustration of the information contained within the copula: A stylized example with two dimensions.

where $\tilde{U} \in \mathbb{R}^{|\mathcal{W}|} \sim \mathbb{C}$. In addition, the function $F_k(\cdot) = \mathbb{Q}_k(\tilde{\xi}_k \leq \cdot)$ represents the cumulative distribution function of element $\tilde{\xi}_k$ of the $|\mathcal{W}|$ -dimensional uncertain vector $\tilde{\xi}$. Note that the probability operator $\mathbb{Q}_k(\cdot)$ represents the marginal distribution function of the random variable $\tilde{\xi}_k$. Therefore, $F_k(\tilde{\xi}_k)$ defines a random variable which is uniformly distributed on the interval $[0, 1]$.

By (3), the resulting distribution of \tilde{U} has marginals that are uniformly distributed on the interval $[0, 1]$ and has the powerful property to embody the dependence between the components of $\tilde{\xi}$. This observation is summarized in Fig. 1 which suggests that the information contained in any multivariate distribution function can be splitted into (i) a collection of marginal distributions (containing the univariate information) and, (ii) a copula (containing the dependence information) from which the univariate information has been filtered.

We now elaborate on the need for a copula-based ambiguity set. Whereas the metric-based ambiguity set \mathcal{M}_1 allows the decision-maker to incorporate useful information as much as possible into the distributionally robust program, it may still contain erroneous distributions, i.e., distributions that do not reflect with fidelity the potential outcome of the uncertainty. For instance, distributions within set \mathcal{M}_1 may exhibit a completely different dependence structure than the one observed empirically. Hence, the decisions may unnecessarily be optimized for an over-conservative and/or non-representative insight of uncertainty, resulting in a higher expected total operational cost. In order to avoid such a situation, we aim to eliminate those distributions from the ambiguity set. In that direction, this paper introduces the copula-based ambiguity set \mathcal{M}_2 which generally contains more representative distribution functions, such that

$$\mathcal{M}_2 = \left\{ \mathbb{Q} \in \mathcal{F} \mid \begin{array}{l} d_W(\mathbb{Q}, \hat{\mathbb{Q}}_N) \leq \theta_1 \\ d_W(\mathbb{C}, \hat{\mathbb{C}}_N) \leq \theta_2 \end{array} \right\}. \quad (4)$$

The first constraint in the ambiguity set \mathcal{M}_2 is identical to the one in \mathcal{M}_1 , yielding the desirable properties of the classical definition of the ambiguity set. The newly added second constraint limits the distributional distance $d_W(\mathbb{C}, \hat{\mathbb{C}}_N)$ between the endogenously selected copula \mathbb{C} of the endogenously

selected distribution \mathbb{Q} and the empirical copula $\widehat{\mathbb{C}}_N$ of the distribution $\widehat{\mathbb{Q}}_N$. This distance should not be greater than $\theta_2 \in \mathbb{R}^+$. Again, θ_2 is a parameter to be tuned by the decision-maker. By restricting the distributions \mathbb{Q} inside the ambiguity set to have a copula \mathbb{C} in the neighbourhood of the empirical one, the distributions inside the ambiguity set will follow a dependence structure which remains close to the historically observed one⁵. Similar to θ_1 , a greater value of θ_2 implies that the decision-maker is less confident about the true dependence structure of the uncertainty, and includes distributions whose dependencies are less similar to those of the empirical one within the ambiguity set.

III. WORST-CASE EXPECTED PROBLEM UNDER THE COPULA-BASED AMBIGUITY SET

By design, DRO aims to determine the *worst-case* distribution within the given ambiguity set, and makes decisions in *expectation* with respect to such a worst-case distribution. This section derives reformulation for a generic distributionally robust worst-case expectation problem, using the copula-based ambiguity set \mathcal{M}_2 . This problem writes as

$$\min_{x \in \mathcal{X}} \overbrace{\max_{\mathbb{Q} \in \mathcal{M}_2} \mathbb{E}^{\mathbb{Q}} \left[a(x)^\top \tilde{\xi} + b(x) \right]}^{\text{Worst-case expected cost}}, \quad (5)$$

where $x \in \mathcal{X}$ is the vector of decision variables. The inner maximization operator in (5) picks the worst-case distribution \mathbb{Q} in the ambiguity set \mathcal{M}_2 . The probability distribution of the uncertain parameter $\tilde{\xi} \in \mathbb{R}^{|\mathcal{W}|}$ is \mathbb{Q} , i.e., $\tilde{\xi} \sim \mathbb{Q}$. The objective function (5) is linear⁶, comprising of the decision-dependent vector $a(x) \in \mathbb{R}^{|\mathcal{W}|}$ and the decision-dependent scalar $b(x) \in \mathbb{R}$.

One key step in deriving the reformulation of (5) is to establish an analytical link between the copula \mathbb{C} and its distribution function \mathbb{Q} . This can be achieved by using (3), in which \mathbb{Q} and \mathbb{C} are linked through the marginal cumulative distribution functions $F_k(\cdot)$. From now on, we denote by $\eta \in \mathbb{R}$, the value of the argument of the function, i.e., $F_k(\eta)$. Let us further clarify this link by a schematic illustration. Fig. 2 shows the shape of the function $F_k(\eta)$ for the renewable power unit k , given the arbitrarily selected eight equiprobable historical observations $\hat{\xi}_{ki}$, $i \in \{1, \dots, N=8\}$ of ξ_k . In particular, this figure shows how the historical observations $\hat{\xi}_{ki}$, the variable η in the x -axis and the function $F_k(\eta)$ in the y -axis are linked. Accordingly, the marginal cumulative distribution function for the renewable power unit k writes as

$$F_k(\eta) = \frac{1}{N} \sum_{i=1}^N \mathbb{1}_{\eta \geq \hat{\xi}_{ki}} \quad \text{with} \quad \mathbb{1}_{\eta \geq \hat{\xi}_{ki}} = \begin{cases} 1 & \text{if } \eta \geq \hat{\xi}_{ki} \\ 0 & \text{otherwise.} \end{cases} \quad (6)$$

⁵Another potential methodology relies on fixing the value of the second-order moment of the distributions within the ambiguity set [19]-[20]. However, the *linear* dependence structure will only be captured by such a constraint. On the contrary, the copula-based approach allows to capture *any* kind of dependence structure (not necessarily linear) and therefore offers a more general framework.

⁶For the sake of simplicity, we assume linearity of the objective function. This assumption is aligned with the current practice of electricity markets with linear bids. An extension to a non-linear objective function is straightforward, but requires additional reformulations that are out of the scope of this paper.

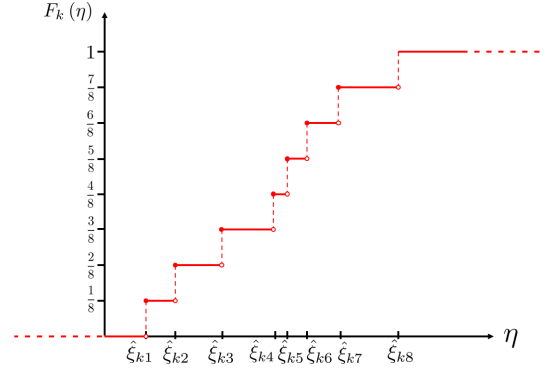


Fig. 2. Illustration of an empirical marginal cumulative distribution function for the renewable power unit k when the number of historical observations is $N = 8$ (an arbitrarily selected number).

Lemma 1. The empirical marginal cumulative distribution function $F_k(\eta)$ for the renewable power unit k is equivalent to the following linear optimization program:

$$\max_{z_{ki}} \frac{1}{N} \sum_{i=1}^N z_{ki} \quad (7a)$$

s.t.

$$z_{ki} (\eta - \hat{\xi}_{ki}) \geq 0 \quad \forall i \in \{1, \dots, N\} \quad (7b)$$

$$0 \leq z_{ki} \leq 1 \quad \forall i \in \{1, \dots, N\}, \quad (7c)$$

where $\eta \in \mathbb{R}$ is the real number that corresponds to the argument of the function and $z_{ki} \in \mathbb{R}^N$ is the decision variable.

Proof. See Appendix A. \square

Based on this analytical link between \mathbb{C} and \mathbb{Q} , it is now possible to reformulate the worst-case expectation problem (5) with the ambiguity set \mathcal{M}_2 .

Remark 1. As notational remark, we write the support as $\{\tilde{\xi} \in \mathbb{R}^{|\mathcal{W}|} \mid C\tilde{\xi} \leq d\}$, where $C \in \mathbb{R}^{2|\mathcal{W}| \times |\mathcal{W}|}$ and $d \in \mathbb{R}^{|\mathcal{W}|}$. The vectors $\tilde{\xi}^{\max} \in \mathbb{R}^{|\mathcal{W}|}$ and $\tilde{\xi}^{\min} \in \mathbb{R}^{|\mathcal{W}|}$ correspond to the maximum and minimum thresholds for the uncertain parameters $\tilde{\xi}$. In the case of renewable energy sources, $\tilde{\xi}^{\min}$ and $\tilde{\xi}^{\max}$ can be zero and the installed capacity, respectively. Note that $C_k \in \mathbb{R}^{2|\mathcal{W}|}$ refers to the k^{th} -row of matrix C . The symbol $a_k(x)$ gives the k^{th} -element of vector $a(x)$. In addition, $F(\hat{\xi}_i) = (F_1(\hat{\xi}_{1i}), \dots, F_k(\hat{\xi}_{ki}), \dots, F_{|\mathcal{W}|}(\hat{\xi}_{|\mathcal{W}|i}))^\top$. The operator $\|\cdot\|_*$ computes the dual norm of a vector.

Theorem 1. Given N historical observations $\hat{\xi}_i$, $i \in \{1, \dots, N\}$ of the random variable ξ , the worst-case expectation problem $\max_{\mathbb{Q} \in \mathcal{M}_2} \mathbb{E}^{\mathbb{Q}} [\Psi(x, \tilde{\xi})]$ is equivalent to the following conic reformulation:

$$\min_{\Pi} \alpha\theta_1 + \beta\theta_2 + \frac{1}{N} \sum_{i=1}^N y_i \quad (8a)$$

$$\text{s.t. } y_i \geq \max_{\xi \in \Xi} \Psi(x, \xi) - \zeta_i^{(1)\top} (\widehat{\xi}_i - \xi) - \zeta_i^{(2)\top} (F(\widehat{\xi}_i) - F(\xi)) \quad \forall i \quad (8b)$$

$$\left\| \zeta_i^{(1)} \right\|_* \leq \alpha \quad \forall i \quad (8c)$$

$$\left\| \zeta_i^{(2)} \right\|_* \leq \beta \quad \forall i, \quad (8d)$$

where $i \in \{1, \dots, N\}$. The decision variables are collected in $\Pi = \{x, \alpha, \beta, y_i, \zeta_i^{(1)}, \zeta_i^{(2)}\}$. In particular, $\alpha, \beta \in \mathbb{R}^+$, $y_i \in \mathbb{R} \quad \forall i \in \{1, \dots, N\}$, and $\zeta_i^{(1)}, \zeta_i^{(2)} \in \mathbb{R}^{|\mathcal{W}|}$ are auxiliary variables. Recall that parameters θ_1 and θ_2 in (8a) are the Wasserstein radii defined for the ambiguity set \mathcal{M}_2 . The vector $F(\xi) = (F_1(\xi_1), \dots, F_{|\mathcal{W}|}(\xi_{|\mathcal{W}|}))^\top$ is reformulated using Lemma 1, and its reformulation is given by

$$F(\xi) = \begin{pmatrix} \left\{ \begin{array}{l} \max_{z_{jki}} \frac{1}{N} \sum_{j=1}^N z_{jki} \\ \text{s.t. } z_{jki} (\xi_k - \widehat{\xi}_{kj}) \geq 0 \quad \forall j \\ 0 \leq z_{jki} \leq 1 \quad \forall j. \end{array} \right\}, k=1 \\ \vdots \\ \left\{ \begin{array}{l} \max_{z_{jki}} \frac{1}{N} \sum_{j=1}^N z_{jki} \\ \text{s.t. } z_{jki} (\xi_k - \widehat{\xi}_{kj}) \geq 0 \quad \forall j \\ 0 \leq z_{jki} \leq 1 \quad \forall j. \end{array} \right\}, k=|\mathcal{W}| \end{pmatrix}. \quad (9)$$

Proof. See Appendix B. \square

The outcome of Theorem 1 is an optimization problem with constraints involving optimization operators, which is not straightforward to be solved by using the off-the-shelf solvers. In Appendix C, we aim to reformulate problem (8), especially constraint (8b), such that it can be incorporated into an optimization problem. This will enable us to reformulate the inner worst-case expectation in (5).

IV. A POWER SYSTEM APPLICATION

Theorem 1 and its tractable solution approach in Appendix C provide a conic reformulation for a general decision-making problem under uncertainty, and therefore it can be applied to any decision-making optimization problem in power systems. As an example, we apply our proposed model to the day-ahead distributionally robust energy and reserve dispatch problem, while capturing the dependencies among renewable energy sources⁷.

⁷In this paper, the power system application is multi-node and single-period. While it correctly models the space restrictions (e.g., via the transmission line capacity constraints), this problem disregards the inter-temporal constraints. Nonetheless, we hypothesize that the extension to a multi-period framework would have limited impact on the final conclusions while tremendously increasing the computational intensity of the problems to be solved. Therefore, for the sake of clarity and simplicity, this extension is left for the future work.

A. The Energy and Reserve Dispatch Problem

Given a generic ambiguity set \mathcal{M} (which is either \mathcal{M}_1 or \mathcal{M}_2 introduced in Section II), the distributionally robust day-ahead energy and reserve dispatch problem reads as

$$\min_{g, \bar{r}, \underline{r}, V} c^\top g + \bar{c}^\top \bar{r} + \underline{c}^\top \underline{r} + \max_{\mathbb{Q} \in \mathcal{M}} \mathbb{E}^{\mathbb{Q}} [c^\top V \tilde{\xi}] \quad (10a)$$

s.t.

$$g + \bar{r} \leq g^{\max} \quad (10b)$$

$$g - \underline{r} \geq g^{\min} \quad (10c)$$

$$0 \leq \underline{r} \leq r^{\max} \quad (10d)$$

$$0 \leq \bar{r} \leq r^{\max} \quad (10e)$$

$$\mathbf{1}^\top g + \mathbf{1}^\top W \mu - \mathbf{1}^\top d = 0 \quad (10f)$$

$$\mathbf{1}^\top V + \mathbf{1}^\top W = 0 \quad (10g)$$

$$\min_{\mathbb{Q} \in \mathcal{M}} \mathbb{Q}(-r_p \leq V_p \tilde{\xi}) \geq 1 - \epsilon_p \quad \forall p \in \mathcal{P} \quad (10h)$$

$$\min_{\mathbb{Q} \in \mathcal{M}} \mathbb{Q}(V_p \tilde{\xi} \leq \bar{r}_p) \geq 1 - \bar{\epsilon}_p \quad \forall p \in \mathcal{P}. \quad (10i)$$

$$\min_{\mathbb{Q} \in \mathcal{M}} \mathbb{Q}(\mathbf{T}_f^{\mathcal{P}}(g + V \tilde{\xi}) + \mathbf{T}_f^{\mathcal{W}} W(\mu + \tilde{\xi}) - \mathbf{T}_f^{\mathcal{D}} d) \leq f_f^{\max} \geq 1 - \epsilon_f \quad \forall f \in \mathcal{F}. \quad (10j)$$

The problem (10) optimizes the day-ahead dispatch $g \in \mathbb{R}^{|\mathcal{P}|}$ of conventional generating units as well as their upward and downward reserve capacity $\bar{r} \in \mathbb{R}^{|\mathcal{P}|}$ and $\underline{r} \in \mathbb{R}^{|\mathcal{P}|}$ to be booked in the day-ahead stage. Objective function (10a) minimizes the total operational cost of the system. The first three terms in (10a) are linear and contains the energy production cost $c \in \mathbb{R}^{|\mathcal{P}|}$ and the upward/downward reserve procurement cost $\bar{c} \in \mathbb{R}^{|\mathcal{P}|}$ and $\underline{c} \in \mathbb{R}^{|\mathcal{P}|}$. The fourth term in (10a), i.e., $\max_{\mathbb{Q} \in \mathcal{M}} \mathbb{E}^{\mathbb{Q}} [c^\top V \tilde{\xi}]$, refers to the operational cost of conventional units, incurred by the activation of their reserve capacity in the real-time operation. This cost is calculated in expectation with respect to the worst-case distribution \mathbb{Q} , which is endogenously selected within the ambiguity set \mathcal{M} . It is approximated by linear decision rules [32] using matrix $V \in \mathbb{R}^{|\mathcal{P}| \times |\mathcal{W}|}$, whose elements are decision variables. Forecast errors $\tilde{\xi} \in \mathbb{R}^{|\mathcal{W}|}$ are in per-unit. Note that the renewable production cost is assumed to be zero.

Constraints (10b) and (10c) ensure that the generation level of conventional units does not exceed their maximum and minimum limits, i.e., $g^{\max} \in \mathbb{R}^{|\mathcal{P}|}$ and $g^{\min} \in \mathbb{R}^{|\mathcal{P}|}$. Constraints (10d) and (10e) enforce the maximum amount of reserve capacity $r^{\max} \in \mathbb{R}^{|\mathcal{P}|}$ that can be provided by conventional units. Constraints (10f) and (10g) ensure the day-ahead and real-time power balance, respectively. In particular, the day-ahead constraint (10f) enforces the sum of total production of conventional generating units $\mathbf{1}^\top g$ and total forecasted production of renewable units $\mathbf{1}^\top W \mu$ to be equal to total demand $\mathbf{1}^\top d$. Note that $d \in \mathbb{R}^{|\mathcal{D}|}$. In addition, $W \in \mathbb{R}^{|\mathcal{W}| \times |\mathcal{W}|}$ is a diagonal matrix of the installed capacity of renewable power units, whereas $\mu \in \mathbb{R}^{|\mathcal{W}|}$ gives their per-unit power generation forecast. The real-time balance in (10g) is ensured via the elements of matrix V , the so-called participation factors, which can be interpreted as follows. The conventional units respond to any deviation in renewable power generation $\tilde{\xi}$ with respect

to the day-ahead forecast μ based on their corresponding participation factors in the matrix V . The recourse action of conventional units is therefore $V\tilde{\xi}$, such that the total recourse action $\mathbb{1}^\top V\tilde{\xi}$ compensates the total renewable power deviation $\mathbb{1}^\top W\tilde{\xi}$. Note that (10g) is an equality constraint, so $\tilde{\xi}$ can be dropped from both sides. In the real-time operation, the recourse action $V\tilde{\xi}$ of conventional units should be limited to the reserve capacities procured in the day-ahead stage, i.e., \bar{r} and \underline{r} . Similarly, the real-time flow within each transmission line $f \in \mathfrak{F}$ should respect the capacity f_f^{\max} . The real-time flows are expressed using the power transfer distribution factor matrices $T_f^P \in \mathbb{R}^{|\mathfrak{F}| \times |\mathcal{P}|}$, $T_f^W \in \mathbb{R}^{|\mathfrak{F}| \times |\mathcal{W}|}$ and $T_f^D \in \mathbb{R}^{|\mathfrak{F}| \times |\mathcal{D}|}$ for conventional generating units, renewable energy sources, and demands, respectively. These restrictions are enforced via probabilistic constraints, namely, Distributionally Robust Chance Constraints (DRCCs) (10h) and (10i) for each conventional generating unit p , and (10j) for each transmission line f . These DRCCs state that the probabilistic constraints within parentheses should be respected under the worst-case distribution \mathbb{Q} within the ambiguity set \mathcal{M} with a probability not lower than $1 - \epsilon$. Note that the value of parameter $\epsilon \in \mathbb{R}$ lies between zero and one, fixed by the power system operator.

B. Reformulation of (10)

The first step is to reformulate DRCCs (10h), (10i) and (10j). For this purpose, we use a Conditional-Value-at-Risk (CVaR) approximation [33]. Consider a DRCC in the form of

$$\min_{\mathbb{Q} \in \mathcal{M}} \mathbb{Q}(\cdot \leq 0) \geq 1 - \epsilon. \quad (11a)$$

In order to get rid of the probability operator $\mathbb{Q}(\cdot)$, the DRCC (11a) can be approximated by the following CVaR constraint:

$$\max_{\mathbb{Q} \in \mathcal{M}} \mathbb{Q}\text{-CVaR}_\epsilon(\cdot) \leq 0. \quad (11b)$$

The CVaR operator in the left-hand side of (11b) is defined as

$$\min_{\tau \in \mathbb{R}} \tau + \frac{1}{\epsilon} \max_{\mathbb{Q} \in \mathcal{M}} \mathbb{E}^{\mathbb{Q}} \left[[\cdot - \tau]^+ \right], \quad (11c)$$

where $\tau \in \mathbb{R}$ is an auxiliary variable. Note that $[\cdot]^+ = \max(\cdot, 0)$. By this approximation, the worst-case expectation problem appears not only in the objective function (10a), but also in every approximated DRCC in the form of (11c). In the following, we provide all reformulations required to solve (10) under both ambiguity sets \mathcal{M}_1 and \mathcal{M}_2 .

1) *Metric-Based Ambiguity Set \mathcal{M}_1* : Reference [15] provides the reformulation of a generic worst-case expectation problem in the form of $\max_{\mathbb{Q} \in \mathcal{M}_1} \mathbb{E}^{\mathbb{Q}} \left[a(x)^\top \tilde{\xi} + b(x) \right]$. Similarly to Theorem 1, this maximization over probability distributions $\mathbb{Q} \in \mathcal{M}_1$ recasts into a minimization problem at the cost of introducing a set of additional auxiliary variables. With this reformulation, the objective function (10a) would contain two min operators that can be merged, yielding a formulation that can be fed into an off-the-shelf solver. Next, we reformulate the worst-case expectation appeared in constraints (10i)

to (10j) after using the CVaR approximation. Following [15], the minimization operators appeared in the constraints can be eventually dropped, but again at the cost of additional auxiliary variables. For the sake of conciseness and completeness, we provide the reformulation of a generic worst-case expectation problem, as well as the final reformulation of problem (10) under ambiguity set \mathcal{M}_1 in the online companion [30].

2) *Copula-Based Ambiguity Set \mathcal{M}_2* : The general procedure to reformulate (10) under ambiguity set \mathcal{M}_2 is similar to the one under set \mathcal{M}_1 . However, instead of following the reformulations in [15], we apply the outcomes of Theorem 1 in Section III. Recall that the solution approach for Theorem 1, proposed in Appendix C, allows us to recast the maximization problem over probability distributions $\mathbb{Q} \in \mathcal{M}_2$ as a minimization problem, but at the cost of additional auxiliary variables. We provide the final reformulation of problem (10) under ambiguity set \mathcal{M}_2 in the online companion [30].

V. CASE STUDY

Our case study is based on a slightly updated version of the 24-node IEEE reliability test system [34], whose input data are provided in the online companion [30]. This case study is composed of 12 conventional generating units with an aggregate capacity of 2,362.5 MW, two wind farms with a total maximum installed capacity of 1,000 MW, and eventually 17 loads with an aggregate demand of 2,207 MW. These power suppliers and demands are connected through a network composed of 24 nodes and 34 transmission lines. The sole source of uncertainty is the deviation of renewable power generation in the real-time operation with respect to the day-ahead forecast values. To cope with such deviations, the system operator reserves a fraction of capacities of conventional units in the day-ahead stage, and activates them in the real-time operation, if necessary. The total maximum reserve capacity that conventional units can provide is 798 MW.

To assess the impacts of dependence structure on operational decisions of the system operator⁸, we generate two distinct datasets of 1,000 samples representing the historical wind power observations. The first one, the so-called *independent dataset*, exhibits no particular dependence structure among uncertain parameters. The second one, the so-called *dependent dataset*, exhibits a dependence structure among uncertain parameters. To generate 1,000 dependent samples, we use the package *DatagenCopulaBased* v1.3.0 in Julia programming language v1.4.2. Both independent and dependent datasets, each with 1,000 samples, and their corresponding copula will be illustrated later in Figs. 4(a) and 4(d), respectively.

A. Procedure of the Out-of-Sample Analysis

Aiming to conduct an ex-post out-of-sample analysis and therefore to compare different models on a fair basis, we split each dataset with 1,000 samples into two different sets of samples. The first one contains 30 samples only (the in-sample

⁸Note that this paper focuses on operational aspects only. The discussion on the way to derive prices for energy and reserves would require advanced analytics which are at the frontier between market design and game theory [35] and are out of the scope of this paper.

data), which are used to characterize the uncertain wind power generation within the models. Therefore, $N = 30$ and indices i and j in (28) run from 1 to 30. The remaining 970 samples in each dataset are used as unseen wind power realizations to assess the quality of operational decisions made in the day-ahead stage.

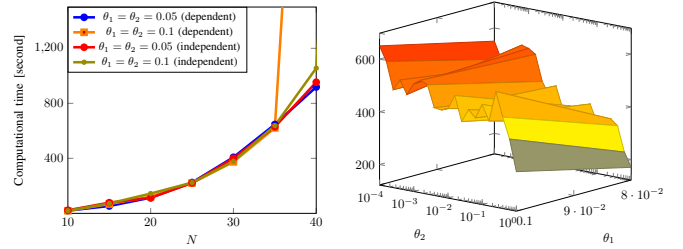
The out-of-sample analysis is as follows. We first solve problem (10) under ambiguity sets \mathcal{M}_1 and \mathcal{M}_2 , both fed with independent and dependent in-sample datasets, and obtain the optimal day-ahead decisions g , r , and \bar{r} . Given fixed values of those day-ahead decisions, we then solve a deterministic optimization problem in the real-time operation for each of 970 unseen samples, whose outcomes are the recourse action of conventional generating units as well as the involuntarily load shedding and the wind curtailment as two extreme recourse actions. The involuntarily load shedding is required when there is a wind power deficit in the real time, but the upward reserve capacities provided by conventional units are insufficient to compensate the entire deficit. Similarly, the wind curtailment occurs when there is a wind power excess in the real time, but there is the lack of downward reserve capacities provided by conventional units to absorb all available wind power. The formulation of this deterministic model is available in the online companion [30]. Once this deterministic optimization problem is solved 970 times for each model and dataset, we calculate the average real-time operational cost of the system. In the rest of this section, we report the out-of-sample cost, which is the sum of operational cost of the system in the day-ahead stage, i.e., the first three terms in (10a), and the average real-time operational cost calculated from the out-of-sample analysis.

B. Computational Performance

All models are solved using Gurobi v8.0.1 in JuMP v0.21.3 under programming language JuliaPro v1.4.2 on a usual computer clocking at 2.2 GHz with 16 GB of RAM. All source codes are publicly available in the online companion [30].

Fig. 3(a) shows the computational time as a function of the number of historical in-sample observations N under different settings. We observe that the computational time increases with the number of historical observations in a non-linear manner. These results suggest that the computational time growth follows a quadratic trend, which is in line with the increase in the number of variables and constraints — see Theorem 1, where the number of certain variables and constraints increases quadratically in N . This quadratic trend is observed irrespective of which dataset (either dependent or independent) is used⁹. In addition, Fig. 3(b) depicts the computational time for various values of parameters θ_1 and θ_2 in the proposed ambiguity set \mathcal{M}_2 . This figure reports the

⁹Compared to other uncertainty modeling techniques, e.g., scenario-based stochastic programming, the DRO approach generally provides more qualified decisions in terms of the out-of-sample performance, when the number of historical in-sample observations is relatively low. This may further motivate the use of DRO when there is limited historical data, or when the decision-maker aims to reduce the computational time by intentionally reducing the number of historical observations. As shown in Fig. 3(a), the computational time for the DRO approach is satisfactory when N is comparatively low.



(a) Computational time as a function of the number of historical in-sample observations N . Both dependent and independent datasets are considered. Fixed value: $\epsilon = 0.05$. (b) Computational time as a function of parameters θ_1 and θ_2 considering the independent dataset. Fixed values: $\epsilon = 0.05$ and $N = 30$.

Fig. 3. Computational study.

computational time considering the independent dataset only, however the trend for the dependent dataset is similar. The results highlight that the computational time slightly decreases when θ_2 increases.

Recall that two wind farms only have been considered so far. We will investigate later in Section V-G the scalability of the proposed model with respect to the dimensionality of the uncertainty space by increasing the number of wind farms.

In the next two subsections, we investigate the out-of-sample performance of the DRO model with the ambiguity sets \mathcal{M}_1 and \mathcal{M}_2 considering both dependent and independent datasets. Recall that the ambiguity set \mathcal{M}_1 contains one risk-tuning parameter only¹⁰, i.e., θ_1 , that restricts the distance of distributions within the ambiguity set to the empirical one. In contrast, the ambiguity set \mathcal{M}_2 comprises of two risk-tuning parameters, i.e., θ_1 and θ_2 , where θ_2 restricts the similarity of distributions within the ambiguity set in terms of the dependence structure to that of the empirical one. For the ease of comparison, we alternately fix one of the two risk-tuning parameters θ_1 and θ_2 , while varying the other one.

C. Out-of-Sample Performance: Operational Cost of the System as a Function of θ_1

We assign three different values to parameter θ_2 , namely 0.01, 0.02, and 0.1, vary the value of parameter θ_1 from 10^{-4} to 10^0 , where the exponent increases linearly with a step of 0.2, and compare the out-of-sample performance of the DRO model with the ambiguity sets \mathcal{M}_1 and \mathcal{M}_2 . We retrieve the average out-of-sample operational cost of the system. In addition, the standard deviation of the cost over 970 out-of-sample simulations is calculated. These results considering both independent and dependent datasets are illustrated in logarithmic Figs. 4(b) and 4(e), respectively.

We first focus on Fig. 4(b) with the independent dataset. One can observe that the results obtained from the DRO model with the ambiguity set \mathcal{M}_1 and those with the ambiguity set \mathcal{M}_2 when θ_2 is comparatively high (e.g., 0.1) are similar. This implies that the second constraint in \mathcal{M}_2 regarding the distance

¹⁰The violation probability $\epsilon_{(j)}$ of each DRCC can also be seen as a risk-tuning parameter. However, we keep this value unchanged (fixed to 0.05) in our numerical study, and focus on the risk-tuning parameters related to the proposed ambiguity set.

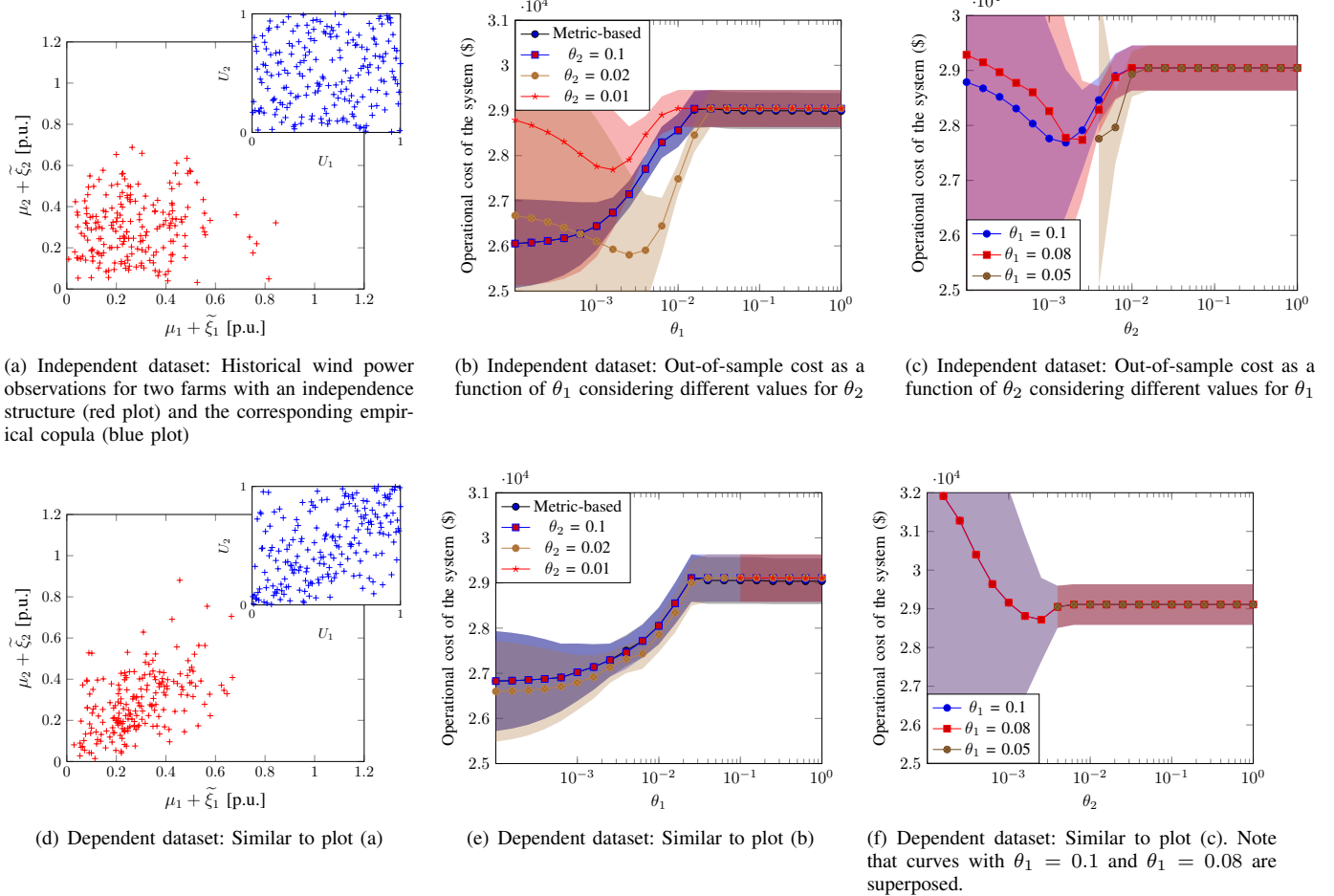


Fig. 4. Numerical study. The shaded area around each curve represents the corresponding standard deviation.

with respect to the empirical copula is not binding, and therefore the worst-case distributions for which the optimal decisions are made are identical in both DRO models. In other words, the ambiguity set \mathcal{M}_2 is identical to \mathcal{M}_1 when θ_2 takes comparatively high values. In contrast, when the value of θ_2 decreases, e.g., to 0.02, the second constraint in \mathcal{M}_2 becomes binding, leading to improved results in terms of the out-of-sample cost. This improvement has led to the lowest out-of-sample cost, since the constraint on dependence structure eliminates the unrealistic distributions from the ambiguity set. This numerical finding suggests that the proposed ambiguity set \mathcal{M}_2 outperforms \mathcal{M}_1 , provided that appropriate values for parameters θ_1 and θ_2 are selected (i.e., $\theta_1 = 0.0025$ and $\theta_2 = 0.02$). Given these appropriate values for θ_1 and θ_2 , we observe a potential cost saving of 1% in expectation with respect to the classical ambiguity set \mathcal{M}_1 given the value for $\theta_1 = 10^{-4}$, which achieves the minimal expected total cost for \mathcal{M}_1 .

We now focus on Fig. 4(e) corresponding to a case with the dependent dataset. We do not observe a significant difference in the results of plots 4(e) and 4(b). The minimum operational cost of the system can still be achieved by the ambiguity set \mathcal{M}_2 , when the values for risk-tuning parameters θ_1 and θ_2 are appropriately selected (e.g., $\theta_1 = 0.0001$ and $\theta_2 = 0.02$,

corresponding to a potential cost saving of 0.9% with respect to the best performance achieved by \mathcal{M}_1). This numerically concludes that the ambiguity set \mathcal{M}_2 has an added value in both cases with independent and dependent datasets. Therefore, irrespective of the dependence structure of the empirical data, a more accurate modeling of the ambiguity set improves the quality of operational decisions.

It is worth mentioning that the DRO model becomes infeasible, when both parameters θ_1 and θ_2 take very low values, meaning that both constraints in \mathcal{M}_2 are highly restrictive. We have observed infeasibility for values of θ_1 and θ_2 lower than 0.01 in our simulations in Section V-C and for values lower than $\theta_1 = 0.05$ and $\theta_2 = 0.004$ in our simulations in Section V-D. The threshold values for θ_1 and θ_2 causing infeasibility in our simulations with independent dataset are close to those with the dependent dataset¹¹. Note that these values are interdependent, meaning that when θ_1 varies, the threshold value for θ_2 also varies. The complete exploration of this frontier would require a high resolution in the mesh of θ_1 and θ_2 , which would in turn require a tremendous computational time. This exploration is therefore left for future extension. One

¹¹Assuming a rapid notification by the solver of an infeasible instance of the program, the decision-maker may have the opportunity to increase the values of parameters θ_1 and θ_2 to restore feasibility.

can intuitively interpret the observation on infeasibility as a case under which the two Wasserstein balls, defined by two constraints in \mathcal{M}_2 , have no intersection. In other words, there is no distribution within the ambiguity set that satisfies both constraints at the same time.

D. Out-of-Sample Performance: Operational Cost of the System as a Function of θ_2

We fix the value of parameter θ_1 to either 0.05, 0.08, or 0.1, and report the out-of-sample operational cost of the system for a varying value of θ_2 . This value is varied from 10^{-4} to 10^0 , where the exponent increases linearly with a step equal to 0.2. Figs. 4(c) and 4(f) show the out-of-sample results for the independent and dependent datasets, respectively.

Our first observation is that for comparatively high values of θ_2 , the outcomes of the DRO model with the ambiguity set \mathcal{M}_2 are very similar to those with the ambiguity set \mathcal{M}_1 . This numerically indicates that the copula constraint is not binding. Second, we observe that the cost curves reach a minimum at intermediate values for θ_2 , suggesting that an optimal value for the parameter θ_2 exists. This difference between the outcomes obtained by the DRO model with \mathcal{M}_1 and those with \mathcal{M}_2 represents the maximum cost saving that is achievable by using \mathcal{M}_2 instead of \mathcal{M}_1 , for fixed value of θ_1 . For instance, in the case of independent dataset when $\theta_1 = 0.1$, the optimum is obtained for $\theta_2 = 0.0016$, and it corresponds to a cost saving of 4.7% compared to \mathcal{M}_1 with the same value of $\theta_1 = 0.1$. Third, we observe that the program becomes infeasible for comparatively low values of θ_2 , when θ_1 is also low (e.g., 0.01), confirming our intuition in the previous analysis.

E. Expected Energy Not Served

We provide a numerical analysis of the Expected Energy Not Served (EENS). The EENS is an indicator that is usually chosen by the system operator to evaluate the amount of load that is expected to be shed during the corresponding time period. In addition to providing an image of the upward reserve constraint violation probability (e.g., an electrical load cannot be supplied in the case where the system operator has not scheduled a sufficient amount of upward operating reserves), this indicator also embeds the information of the severity of the constraint violation. We calculate the EENS under the case of the independent dataset, for $\epsilon = 0.05$, and provide the results in Fig. 6.

The left-hand side plot 6(a) compares the EENS between the benchmark (i.e., the traditional metric-based ambiguity set \mathcal{M}_1) and the proposed modeling approach \mathcal{M}_2 when θ_1 ranges from 10^{-4} to 10^{-1} and for different arbitrarily fixed values for $\theta_2 = \{0.01, 0.02, 0.1\}$. First, we observe that the EENS curves are similar for the traditional metric-based model based on \mathcal{M}_1 and the proposed modeling approach \mathcal{M}_2 , when θ_2 takes a comparatively high value (e.g., $\theta_2 = 0.1$). This confirms the observation discussed in Section V.C, which suggests that the proposed modeling approach provides similar performance as that of \mathcal{M}_1 when the constraint on copula is not binding. Second, we observe that the EENS decreases and tends to zero when the value of θ_1 increases. Recall that the Wasserstein

radius θ_1 relates to the distributional robustness. This means that, when θ_1 increases, the number of plausible distributions within the set increases, ensuing a potentially more conservative worst-case distribution. This, in turn, impacts the empirical violation probabilities (and therefore, the EENS), because the violation probability ϵ has not the same meaning when evaluated for different distributions.

The right-hand side plot 6(b) compares the evolution of EENS when θ_2 increases for different arbitrarily selected values of $\theta_1 = \{0.05, 0.08, 0.1\}$. Similarly, we observe that the EENS tends to decrease when θ_2 increases. One may interpret this result as follows. When the copula constraint is not binding (i.e., θ_2 is comparatively high), the results tend to those obtained from the traditional DRO with the corresponding value for θ_1 . However, when the constraint is binding (i.e., θ_2 takes a lower value), the optimal decisions are less conservative, because the distributions within the set are restricted to follow a dependence structure which is close to that contained in the empirical distribution, resulting in a potentially higher EENS. In other words, robust decisions are made against a realistic dependence structure instead of any type of dependence structure.

F. Operational Decisions

We explore the impacts of the proposed ambiguity set \mathcal{M}_2 on the resulting operational decisions. Fig. 5(a) reports the total upward reserve capacity, i.e., $\mathbb{1}^\top \bar{r}$, procured from conventional units in the day-stage stage considering both independent and dependent datasets. In particular, we solve the DRO model under three different settings: (i) with the ambiguity set \mathcal{M}_1 , (ii) with the ambiguity set \mathcal{M}_2 where $\theta_2 = 0.001$, and (iii) with the ambiguity set \mathcal{M}_2 where $\theta_2 = 0.1$. In all three cases, we fix the value of θ_1 to be 0.1. We observe that when θ_2 takes a comparatively higher value (i.e., 0.1), the resulting operational decisions obtained from the DRO model with the ambiguity set \mathcal{M}_2 are identical to those with the ambiguity set \mathcal{M}_1 . This confirms our earlier observation that the copula constraint in \mathcal{M}_2 is non-binding. On the contrary, when the parameter θ_2 is given an appropriate value (here, e.g., 0.001), not only the out-of-sample cost (see Figs. 4(c) and 4(f)) but also the total amount of reserve capacity (see Fig. 5(a)) decreases. This interesting observation implies that by elegantly incorporating the dependence structure into the ambiguity set definition, the DRO model will provide *less* conservative operational decisions.

G. Impacts of Increasing the Number of Wind Farms

We increase the number of wind farms connected to the system, enlarging the dimension of the uncertainty space. We rescale the wind farm capacities, such that the aggregate capacity of wind farms is always equal to 1,000 MW. We consider 15 historical observations with dependence structure¹².

¹²The number of in-sample scenarios have been reduced in the scope of this scalability study, to keep reasonable computational time in the most extreme cases (e.g., when 12 wind farms are considered). Recall that the computational tractability of the program is related to the dimension of the input data, i.e., N scenarios of dimension $|\mathcal{W}|$.

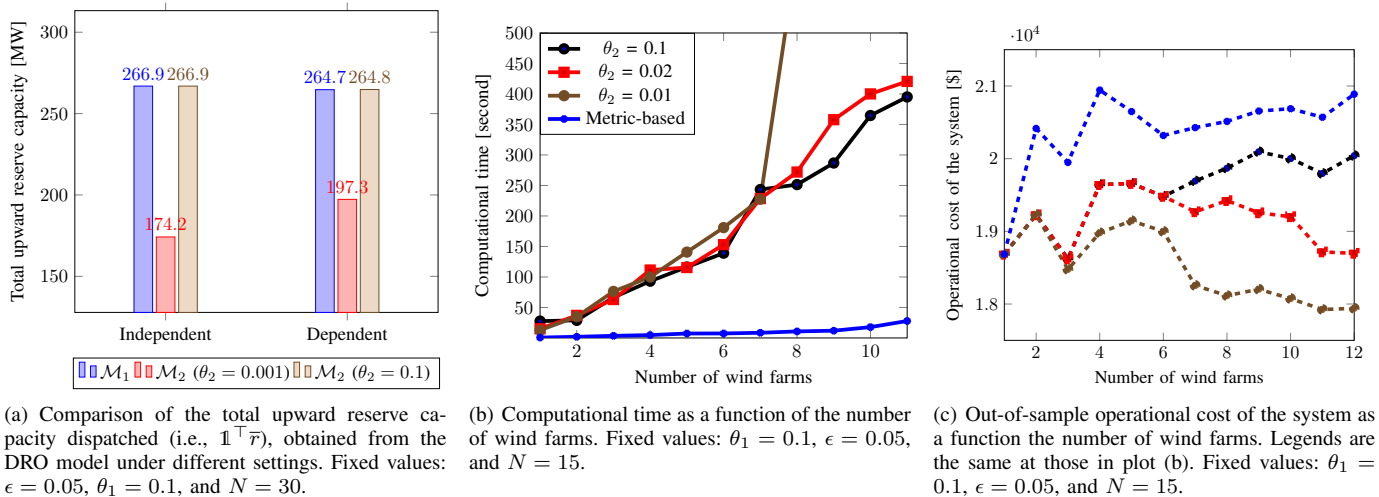


Fig. 5. Operational results with two (the first plot) and more (the next two plots) wind farms. The aggregate capacity of farms is always equal to 1,000 MW.

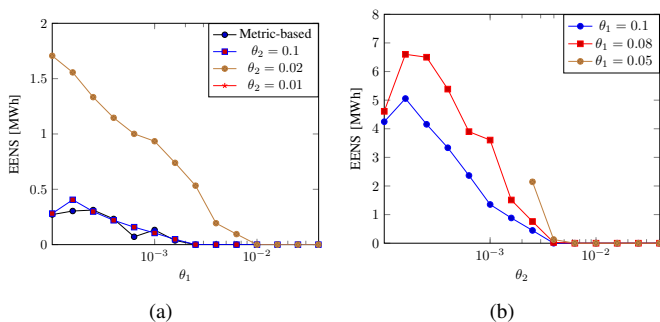


Fig. 6. Expected energy not served (EENS) as a function of θ_1 and θ_2 under the independent dataset (fixed values: $N = 30$, $\epsilon = 0.05$).

Fig. 5(b) shows the computational time to solve the problem (10) with both ambiguity sets \mathcal{M}_1 (metric-based) and \mathcal{M}_2 (with different values of θ_2). The value of parameter θ_1 is fixed to 0.1 in all cases. In most cases, the computational time increases linearly with the number of wind farms. However, this increase is drastic when the value of θ_2 is comparatively low, indicating the case with a tight copula constraint. We hypothesize that this increase is related to an instance of the problem which is close to the infeasibility threshold discussed in Section V.D. Dedicated decomposition algorithms may help handle this computational problem [36], but their implementation remains out of the scope of this paper.

Fig. 5(c) illustrates the out-of-sample operational cost of the system as a function of the number of wind farm. Legends are the same as those in Fig. 5(b). There are two important observations. First, we obtain lower values for the operational cost under the ambiguity set \mathcal{M}_2 , in particular when the value of θ_2 is comparatively low, e.g., 0.01 or 0.02. Second, the operational cost decreases by increasing the number of wind farms, provided that the value of θ_2 is comparatively low. Both observations highlight the importance of adding dependence structure in the definition of the ambiguity set, particularly when the number of wind farms is comparatively high.

VI. CONCLUSION

This paper goes beyond the current state of the art and introduces an ambiguity set that includes an additional Wasserstein constraint on copula, therefore capturing the whole dependence structure among all uncertain parameters. We develop a generic distributionally robust model that can be applied to any kind of decision-making optimization problems in power systems under uncertainty. In particular, we apply the proposed model to a distributionally robust day-ahead energy and reserve dispatch problem. The results show the potential for a significant operational cost saving for the whole system, achieved by taking into account the dependence structure of the uncertain renewable energy sources.

As a potential path for future research, the development of a tool, e.g., using machine learning techniques, that determines *a priori* the optimal values of parameters θ_1 and θ_2 may help the decision-maker efficiently use the proposed model. The study of the feasibility region of the proposed formulation in terms of θ_1 and θ_2 can be insightful for deeper understanding their underlying relation. In addition, the research towards an exact reformulation of Theorem 1 may lead to an improved performance in terms of the out-of-sample operational cost of the system. A potential added value to the proposed modeling approach would require to endogenously model the marginal cumulative distribution functions of the variable distributions within the ambiguity set. This would relax the restrictive assumption discussed in Footnote 14, and may increase the flexibility of the proposed modeling approach. Finally, it is interesting to apply the outcome of Theorem 1 to various short-term operational and long-term planning decision-making problems under uncertainty in power systems to further illustrate the potential benefits of the proposed model.

APPENDIX A PROOF OF LEMMA 1

Proof. For a given argument value η , the program counts the number of historical observations $\hat{\xi}_{ki}$, $i \in \{1, \dots, N\}$

corresponding to the renewable power unit k under which the renewable power generation is lower than η . The constraint (7b) imposes that the variable z_{ki} takes a non-negative value whenever η is higher than the underlying observation $\widehat{\xi}_{ki}$, and vice versa. However, the value of z_{ki} is restricted to lie within 0 and 1 in (7c). Therefore, the optimal value of z_{ki} will mimic the function $\mathbb{1}_{\eta \geq \widehat{\xi}_{ki}}$. This enables the objective function (7a) to compute the value of the empirical marginal cumulative distribution function. \square

APPENDIX B PROOF OF THEOREM 1

Proof. We depart from the worst-case expectation problem

$$\max_{\mathbb{Q} \in \mathcal{M}_2} \mathbb{E}^{\mathbb{Q}} \left[\Psi(x, \tilde{\xi}) \right], \quad (12)$$

where \mathbb{Q} is the variable distribution function and $\Psi(x, \tilde{\xi}) = a(x)^\top \tilde{\xi} + b(x)$ represents the linear objective function, which depends on outer decision variables $x \in \mathcal{X}$. The problem seeks the distribution within the ambiguity set \mathcal{M}_2 , defined by (4), which maximizes the objective function in expectation. This problem can be developed as follows:

$$\max_{\mathbb{Q}} \mathbb{E}^{\mathbb{Q}} \left[\Psi(x, \tilde{\xi}) \right] \quad (13a)$$

$$\text{s.t. } d_W(\mathbb{Q}, \widehat{\mathbb{Q}}_N) \leq \theta_1 \quad (13b)$$

$$d_W(\mathbb{C}, \widehat{\mathbb{C}}_N) \leq \theta_2. \quad (13c)$$

From now on, for the sake of clarity, we assume that distribution \mathbb{Q} is discrete. Note that it is straightforward to extend the proof for continuous distribution functions. Note also that this assumption will be relaxed in the following developments, making the final result valid for continuous distributions as well. Given a set of fixed samples ξ_l (e.g., a mesh of the support of uncertainty) with $l \in \{1, \dots, L\}$, where L is an arbitrarily large number, the variable distribution \mathbb{Q} is defined by

$$\mathbb{Q} = \sum_{l=1}^L \mathbb{Q}_l \delta_{\xi_l}, \quad (14)$$

where \mathbb{Q}_l is the variable probability affected to sample ξ_l , and δ_{ξ_l} is the Dirac distribution centered on ξ_l . We are now able to reformulate (22) into

$$\max_{\mathbb{Q}_l} \sum_{l=1}^L \Psi(x, \xi_l) \mathbb{Q}_l \quad (15a)$$

$$\text{s.t. } \left\{ \begin{array}{l} \min_{\pi_{li}^{(1)}} \sum_{l=1}^L \sum_{i=1}^N d(\widehat{\xi}_i, \xi_l) \pi_{li}^{(1)} \\ \text{s.t. } \sum_{l=1}^L \pi_{li}^{(1)} = (\widehat{\mathbb{Q}}_N)_i \quad \forall i \in \{1, \dots, N\} \\ \sum_{i=1}^N \pi_{li}^{(1)} = \mathbb{Q}_l \quad \forall l \in \{1, \dots, L\} \end{array} \right\} \leq \theta_1 \quad (15b)$$

$$\left\{ \begin{array}{l} \min_{\pi_{li}^{(2)}} \sum_{l=1}^L \sum_{i=1}^N d_F(\widehat{\xi}_i, \xi_l) \pi_{li}^{(2)} \\ \text{s.t. } \sum_{l=1}^L \pi_{li}^{(2)} = (\widehat{\mathbb{C}}_N)_i \quad \forall i \in \{1, \dots, N\} \\ \sum_{i=1}^N \pi_{li}^{(2)} = \mathbb{C}_l \quad \forall l \in \{1, \dots, L\} \end{array} \right\} \leq \theta_2, \quad (15c)$$

where the expectation in the objective function has been developed for distribution \mathbb{Q} , and the Wasserstein distances $d_W(\mathbb{Q}, \widehat{\mathbb{Q}}_N)$ and $d_W(\mathbb{C}, \widehat{\mathbb{C}}_N)$ have been reformulated according to their mathematical definitions. The variables $\pi_{li}^{(1)} \in \mathbb{R}^{L \times N}$ and $\pi_{li}^{(2)} \in \mathbb{R}^{L \times N}$ represent the optimal transportation plan between distributions $\widehat{\mathbb{Q}}_N$ and \mathbb{Q} , and $\widehat{\mathbb{C}}_N$ and \mathbb{C} , respectively. The distance functions $d(\widehat{\xi}_i, \xi_l)$ and $d_F(\widehat{\xi}_i, \xi_l)$ will be defined later on within the proof.

We reformulate (15) via three steps. First, we observe that the probabilities $(\widehat{\mathbb{P}}_N)_i = (\widehat{\mathbb{C}}_N)_i = \frac{1}{N} \forall i \in \{1, \dots, N\}$ and $\mathbb{Q}_l = \mathbb{C}_l \forall l \in \{1, \dots, L\}$. Next, we are able to drop the minimization operators since they appear in a “less-or-equal-to” constraint and to add the variables $\pi_{li}^{(1)}$ and $\pi_{li}^{(2)}$ to the set of overall variables. Finally, we drop variables \mathbb{Q}_l by (i) substituting its expression in the third equation of (15b) into the objective function, and (ii) adding the constraint $\sum_{i=1}^N \pi_{li}^{(1)} = \sum_{i=1}^N \pi_{li}^{(2)} \forall l \in \{1, \dots, L\}$, which translates $\mathbb{Q}_l = \mathbb{C}_l \forall l \in \{1, \dots, L\}$. We end up in

$$\max_{\pi_{li}^{(1)}, \pi_{li}^{(2)}} \sum_{l=1}^L \sum_{i=1}^N \Psi(x, \xi_l) \pi_{li}^{(1)} \quad (16a)$$

$$\text{s.t. } \sum_{l=1}^L \sum_{i=1}^N d(\widehat{\xi}_i, \xi_l) \pi_{li}^{(1)} \leq \theta_1 : \alpha \quad (16b)$$

$$\sum_{l=1}^L \pi_{li}^{(1)} = \frac{1}{N} \forall i \in \{1, \dots, N\} : y_i \quad (16c)$$

$$\sum_{l=1}^L \sum_{i=1}^N d_F(\widehat{\xi}_i, \xi_l) \pi_{li}^{(2)} \leq \theta_2 : \beta \quad (16d)$$

$$\sum_{l=1}^L \pi_{li}^{(2)} = \frac{1}{N} \forall i \in \{1, \dots, N\} : t_i \quad (16e)$$

$$\sum_{i=1}^N \pi_{li}^{(1)} = \sum_{i=1}^N \pi_{li}^{(2)} \forall l \in \{1, \dots, L\} : \sigma_l, \quad (16f)$$

where $\{\alpha, \beta, y_i, t_i, \sigma_l\}$ is the set of dual variables. Next, we dualize (16), yielding

$$\min_{\alpha \geq 0, \beta \geq 0, y_i, t_i, \sigma_l} \alpha \theta_1 + \beta \theta_2 + \frac{1}{N} \sum_{i=1}^N y_i + \frac{1}{N} \sum_{i=1}^N t_i \quad (17a)$$

$$\text{s.t. } y_i \geq \Psi(x, \xi_l) - \alpha d(\widehat{\xi}_i, \xi_l) + \sigma_l \quad \forall i, \forall l \quad (17b)$$

$$t_i \geq -\beta d_F(\widehat{\xi}_i, \xi_l) - \sigma_l \quad \forall i, \forall l. \quad (17c)$$

The constraints in (17) can be equivalently reformulated using maximization operators:

$$\min_{\alpha \geq 0, \beta \geq 0, y_i, t_i, \sigma_l} \alpha \theta_1 + \beta \theta_2 + \frac{1}{N} \sum_{i=1}^N y_i + \frac{1}{N} \sum_{i=1}^N t_i \quad (18a)$$

$$\text{s.t. } y_i \geq \max_{\xi_i, \sigma_l} \Psi(x, \xi_i) - \alpha d(\widehat{\xi}_i, \xi_i) + \sigma_l \quad \forall i \quad (18b)$$

$$t_i \geq \max_{\xi_i, \sigma_l} -\beta d_F(\widehat{\xi}_i, \xi_i) - \sigma_l \quad \forall i. \quad (18c)$$

The maximization operators in (18b) and (18c) can be moved to the objective function, while dropping auxiliary variables y_i and t_i . The summation and maximization operators are merged such that the variable σ_l simplifies. Furthermore, we relax the assumption on discrete set of sample ξ_l by introducing a continuous support of uncertainty $\Xi = \{\xi \in \Xi \mid C\xi \leq d\}$. Finally, for the ease of developments, we re-introduce auxiliary variable y_i , such that (18) is equivalent to

$$\min_{\alpha, \beta \geq 0, y_i} \alpha \theta_1 + \beta \theta_2 + \frac{1}{N} \sum_{i=1}^N y_i \quad (19a)$$

$$\text{s.t. } y_i \geq \max_{\xi \in \Xi} \Psi(x, \xi) - \alpha d(\widehat{\xi}_i, \xi) - \beta d_F(\widehat{\xi}_i, \xi) \quad \forall i. \quad (19b)$$

Note that (19) is equivalent to the findings in [27, Theorem 2]. The complicating part in (19) is the constraint (19b), as it contains a maximization operator over variable ξ and the distance functions, which are defined in the following. From now on, the proof will focus on the reformulation of (19b). The distance functions are defined using norms, such that

$$d(\widehat{\xi}_i, \widetilde{\xi}) = \|\widehat{\xi}_i - \widetilde{\xi}\|, \quad (20a)$$

and

$$d_F(\widehat{\xi}_i, \widetilde{\xi}) = \|F(\widehat{\xi}_i) - F(\widetilde{\xi})\|, \quad (20b)$$

where $F(\widehat{\xi}_i) = (F_1(\widehat{\xi}_{1i}), \dots, F_k(\widehat{\xi}_{ki}), \dots, F_{|\mathcal{W}|}(\widehat{\xi}_{|\mathcal{W}|i}))^\top$ and $F(\widetilde{\xi}) = (F_1(\widetilde{\xi}_1), \dots, F_k(\widetilde{\xi}_k), \dots, F_{|\mathcal{W}|}(\widetilde{\xi}_{|\mathcal{W}|}))^\top$ are vectors in $\mathbb{R}^{|\mathcal{W}|}$. In other words, each component of $\widehat{\xi}_i$ or $\widetilde{\xi}$ is given as argument of its corresponding marginal cumulative distribution function. Note that the resulting vector $F(\widehat{\xi}_i)$ is a sample of the copula, which can be evaluated *a priori* using (3). Note also that $F(\widetilde{\xi})$ is a decision variable related to the variations within the variable copula, which requires further reformulations. Using such distance definitions, (19b) can be recast into

$$y_i \geq \max_{\xi \in \Xi} \Psi(x, \widetilde{\xi}) - \alpha \|\widehat{\xi}_i - \widetilde{\xi}\| - \beta \|F(\widehat{\xi}_i) - F(\widetilde{\xi})\| \quad \forall i. \quad (21)$$

To get rid of the norms inside the objective function of the inner maximization problem, we use dual norms ($\|x\|_* = \max_{\|v\| \leq 1} v^\top x$) as

$$y_i \geq \max_{\xi \in \Xi} \Psi(x, \widetilde{\xi}) - \alpha \max_{\|\zeta_i^{(1)}\|_* \leq 1} \zeta_i^{(1)\top} (\widehat{\xi}_i - \widetilde{\xi})$$

$$- \beta \max_{\|\zeta_i^{(2)}\|_* \leq 1} \zeta_i^{(2)\top} (F(\widehat{\xi}_i) - F(\widetilde{\xi})) \quad \forall i. \quad (22)$$

Next, we eliminate the maximization operators on variables $\zeta_i^{(1)}$ and $\zeta_i^{(2)}$ by (i) switching the $-\max$ to a \min , (ii) moving the resulting minimization operators to the left, (iii) merging the min operators over variables $\zeta_i^{(1)}$ and $\zeta_i^{(2)}$, (iv) permuting with the max operator over $\widetilde{\xi}$ (which is allowed because the objective function is linear¹³ and the feasible sets are convex and independent), and finally (v) dropping the min operator from the right-hand side of the \geq constraint. The variables $\zeta_i^{(1)}$ and $\zeta_i^{(2)}$ are added to the overall set of decision variables and the constraints are added to the overall set of constraints, such that

$$y_i \geq \max_{\xi \in \Xi} \Psi(x, \widetilde{\xi}) - \alpha \zeta_i^{(1)\top} (\widehat{\xi}_i - \widetilde{\xi}) - \beta \zeta_i^{(2)\top} (F(\widehat{\xi}_i) - F(\widetilde{\xi})) \quad \forall i \quad (23a)$$

$$\|\zeta_i^{(1)}\|_* \leq 1 \quad \forall i \quad (23b)$$

$$\|\zeta_i^{(2)}\|_* \leq 1 \quad \forall i, \quad (23c)$$

is equivalent to (19b). With the changes of variables $\alpha \zeta_i^{(1)} \rightarrow \zeta_i^{(1)}$ and $\beta \zeta_i^{(2)} \rightarrow \zeta_i^{(2)}$, the constraints become

$$y_i \geq \max_{\xi \in \Xi} \Psi(x, \xi) - \zeta_i^{(1)\top} (\xi_i - \xi) - \zeta_i^{(1)\top} (F(\xi_i) - F(\xi)) \quad \forall i \quad (24a)$$

$$\|\zeta_i^{(1)}\|_* \leq \alpha \quad \forall i \quad (24b)$$

$$\|\zeta_i^{(2)}\|_* \leq \beta \quad \forall i. \quad (24c)$$

We use Lemma 1 to reformulate the variable function $F(\xi)$. This key step allows us to make the link between the sample displacements in the variable distribution and the sample displacement in the variable copula¹⁴. The vector $F(\xi)$ now becomes (9) which completes the proof. \square

APPENDIX C SOLUTION APPROACH

We aim to reformulate problem (8), especially constraint (8b). The first step of the reformulation consists in getting rid

¹³Note that the objective function contains the variable vector $F(\widetilde{\xi})$, which corresponds to the collection of marginal cumulative distribution functions. In the general case where the marginal cumulative distribution functions are non-convex, the permutation between min and max operators is not allowed. However, in the setting of this paper, the vector $F(\widetilde{\xi})$ is reformulated using the empirical marginal cumulative distribution functions modeled via Lemma 1, which refers to a linear and convex optimization problem. Therefore, the permutation between min and max operators is allowed.

¹⁴It is worth mentioning that Lemma 1 defines the shape of the empirical marginal cumulative distribution functions $F_k(\eta) \quad \forall k$. We therefore use the same marginals in the formulation of the empirical copula $\widehat{\mathbb{C}}_N$ and the variable copula \mathbb{C} . This assumption implicitly implies that the distributions \mathbb{Q} and $\widehat{\mathbb{Q}}_N$ follow the same marginal distributions. In turn, this may restrict the flexibility of the proposed DRO approach as it requires the distributions within the ambiguity set to follow discrete marginals. Nonetheless, the numerical results suggest that, even under this assumption, the proposed modeling approach benefits the decision-maker by taking the advantage of the available dependence information.

of the maximization operators within $F(\xi)$. In that direction, we derive the optimality conditions related to the optimization problems in (9) and add them into the constraints of the outer maximization problem. We observe that the underlying optimization problems verify the Slater condition. Therefore, the necessary and sufficient optimality conditions for the k -th element of vector $F(\xi)$ in (9) are composed of (i) the primal constraints, (ii) the dual constraints, and (iii) the strong duality equality. This mathematically translates to the following set of constraints:

$$z_{jki} \left(\xi_k - \widehat{\xi}_{kj} \right) \geq 0 \quad \forall j \quad (25a)$$

$$0 \leq z_{jki} \leq 1 \quad \forall j \quad (25b)$$

$$\frac{1}{N} + \sigma_{kji} \left(\xi_k - \widehat{\xi}_{kj} \right) - \pi_{kji} \leq 0 \quad \forall j \quad (25c)$$

$$\sigma_{kji}, \pi_{kji} \geq 0 \quad \forall j \quad (25d)$$

$$\frac{1}{N} \sum_{j=1}^N z_{kji} = \sum_{j=1}^N \pi_{kji}. \quad (25e)$$

By doing so, the constraint (8b) becomes

$$y_i \geq \left\{ \begin{array}{l} \max_{\xi, z_{kji}, \sigma_{kji}, \pi_{kji}} \Psi(x, \xi) - \zeta_i^{(1)\top} \left(\widehat{\xi}_i - \xi \right) \\ - \zeta_i^{(2)\top} \left(F \left(\widehat{\xi}_i \right) - \frac{1}{N} \begin{pmatrix} \sum_{j=1}^N z_{j1i} \\ \vdots \\ \sum_{j=1}^N z_{j|\mathcal{W}|i} \end{pmatrix} \right) \\ \text{s.t. } C\xi \leq d \\ z_{jki} \left(\xi_k - \widehat{\xi}_{kj} \right) \geq 0 \quad \forall k, j \\ 0 \leq z_{jki} \leq 1 \quad \forall k, j \\ \frac{1}{N} + \sigma_{kji} \left(\xi_k - \widehat{\xi}_{kj} \right) - \pi_{kji} \leq 0 \quad \forall k, j \\ \sigma_{kji}, \pi_{kji} \geq 0 \quad \forall k, j \\ \frac{1}{N} \sum_{j=1}^N z_{kji} = \sum_{j=1}^N \pi_{kji} \quad \forall k \end{array} \right\} \quad \forall i, \quad (26a)$$

where the inner maximization operator has been dropped and the optimality conditions have been added to the set of constraints of the outer maximization problem. We notice that the resulting outer maximization problem contains bilinear terms in the form of $z_{jki}\xi_k$ and $\sigma_{kji}\xi_k$. We use the McCormick relaxation of bilinear terms to restore linearity, such that the constraint can be cast into

$$y_i \geq \left\{ \begin{array}{l} \max_{\xi, z_{kji}, \sigma_{kji}, \pi_{kji}} \Psi(x, \xi) - \zeta_i^{(1)\top} \left(\widehat{\xi}_i - \xi \right) \\ - \zeta_i^{(2)\top} \left(F \left(\widehat{\xi}_i \right) - \frac{1}{N} \begin{pmatrix} \sum_{j=1}^N z_{j1i} \\ \vdots \\ \sum_{j=1}^N z_{j|\mathcal{W}|i} \end{pmatrix} \right) \\ \text{s.t. } C\xi \leq d \\ t_{jki} - z_{jki}\widehat{\xi}_{kj} \geq 0 \quad \forall k, j \\ t_{jki} \geq z_{jki}\xi_k^{\min} \quad \forall k, j \\ t_{jki} \geq \xi_k + z_{kji}\xi_k^{\max} - \xi_k^{\max} \quad \forall k, j \\ t_{jki} \leq \xi_k + z_{kji}\xi_k^{\min} - \xi_k^{\min} \quad \forall k, j \\ t_{jki} \geq z_{jki}\xi_k^{\max} \quad \forall k, j \\ 0 \leq z_{jki} \leq 1 \quad \forall k, j \\ \frac{1}{N} + v_{jki} - \sigma_{kji}\widehat{\xi}_{kj} - \pi_{kji} \leq 0 \quad \forall k, j \\ v_{jki} \geq \sigma_{kji}\xi_k^{\min} \quad \forall k, j \\ v_{jki} \geq \overline{V}\xi_k + \sigma_{kji}\xi_k^{\max} - \overline{V}\xi_k^{\max} \quad \forall k, j \\ v_{jki} \leq \overline{V}\xi_k + \sigma_{kji}\xi_k^{\min} - \overline{V}\xi_k^{\min} \quad \forall k, j \\ v_{jki} \geq \sigma_{kji}\xi_k^{\max} \quad \forall k, j \\ \sigma_{kji}, \pi_{kji} \geq 0 \quad \forall k, j \\ \frac{1}{N} \sum_{j=1}^N z_{kji} = \sum_{j=1}^N \pi_{kji} \quad \forall k \end{array} \right\} \quad \forall i. \quad (27a)$$

We now focus on getting rid of the outer maximization operator. The final step of the reformulation is to dualize (27), such that the problem becomes a minimization and the operator can be dropped from the constraint. The following problem is a tractable reformulation of (8):

$$\min_{\Pi} \alpha\theta_1 + \beta\theta_2 + \frac{1}{N} \sum_{i=1}^N y_i \quad (28a)$$

$$\text{s.t. } y_i \geq b(x) - \zeta_i^{(1)\top} \widehat{\xi}_i - \zeta_i^{(2)\top} F \left(\widehat{\xi}_i \right) + \mu^{(0)\top} d \\ + \sum_{k=1}^{|\mathcal{W}|} \sum_{j=1}^N \left(\mu_{kji}^{(3)} \widetilde{\xi}_k^{\max} - \mu_{kji}^{(4)} \widetilde{\xi}_k^{\min} + \mu_{kji}^{(6)} + \frac{1}{N} \mu_{kji}^{(7)} + \mu_{kji}^{(9)} \overline{V} \xi_k^{\max} - \mu_{kji}^{(10)} \overline{V} \xi_k^{\min} \right) \quad \forall i \quad (28b)$$

$$a_k(x) + \zeta_{ik}^{(1)} - C_k^\top \mu^{(0)} \\ + \sum_{j=1}^N \left(\mu_{kji}^{(3)} + \mu_{kji}^{(4)} + \overline{V} \mu_{kji}^{(10)} - \overline{V} \mu_{kji}^{(9)} \right) = 0 \quad \forall k, i \quad (28c)$$

$$\frac{1}{N} \zeta_{ik}^{(2)} - \mu_{kji}^{(1)} \widehat{\xi}_{kj} - \mu_{kji}^{(2)} \widetilde{\xi}_k^{\min} - \mu_{kji}^{(3)} \widetilde{\xi}_k^{\max} \\ + \mu_{kji}^{(4)} \widetilde{\xi}_k^{\min} + \mu_{kji}^{(5)} \widetilde{\xi}_k^{\max} - \mu_{kji}^{(6)} + \frac{1}{N} \lambda_k \leq 0 \quad \forall k, j, i \quad (28d)$$

$$\mu_{kji}^{(1)} + \mu_{kji}^{(2)} + \mu_{kji}^{(3)} - \mu_{kji}^{(4)} - \mu_{kji}^{(5)} = 0 \quad \forall k, j, i \quad (28e)$$

$$- \mu_{kji}^{(7)} + \mu_{kji}^{(8)} + \mu_{kji}^{(9)} - \mu_{kji}^{(10)} - \mu_{kji}^{(11)} = 0 \quad \forall k, j, i \quad (28f)$$

$$\mu_{kji}^{(7)} - \lambda_k = 0 \quad \forall k, j, i \quad (28g)$$

$$\mu_{kji}^{(7)} - \mu_{kji}^{(8)} \xi_k^{\min} - \mu_{kji}^{(9)} \xi_k^{\max} + \mu_{kji}^{(10)} \xi_k^{\min} + \mu_{kji}^{(11)} \xi_k^{\max} \leq 0 \quad \forall k, j, i \quad (28h)$$

$$\left\| \zeta_i^{(1)} \right\|_* \leq \alpha \quad \forall i \quad (28i)$$

$$\left\| \zeta_i^{(2)} \right\|_* \leq \beta \quad \forall i. \quad (28j)$$

REFERENCES

- [1] The North American Electric Reliability Corporation (NERC), "Special report: Potential reliability impacts of emerging flexible resources," 2010, [Online]. Available: https://www.nerc.com/files/IVGTF_Task_1_5_Final.pdf.
- [2] J. M. Morales, A. J. Conejo, H. Madsen, P. Pinson, and M. Zugno, *Integrating Renewables in Electricity Markets*. Springer, 2013.
- [3] J. M. Morales, A. J. Conejo, and J. Perez-Ruiz, "Economic valuation of reserves in power systems with high penetration of wind power," *IEEE Trans. Power Syst.*, vol. 24, no. 2, pp. 900–910, 2009.
- [4] V. M. Zavala, K. Kim, M. Anitescu, and J. Birge, "A stochastic electricity market clearing formulation with consistent pricing properties," *Oper. Res.*, vol. 65, no. 3, pp. 557–576, 2017.
- [5] D. Bertsimas, E. Litvinov, X. A. Sun, J. Zhao, and T. Zheng, "Adaptive robust optimization for the security constrained unit commitment problem," *IEEE Trans. Power Syst.*, vol. 28, no. 1, pp. 52–63, 2013.
- [6] M. Zugno and A. J. Conejo, "A robust optimization approach to energy and reserve dispatch in electricity markets," *Eur. J. Oper. Res.*, vol. 247, pp. 659–671, 2015.
- [7] D. Bienstock, M. Chertkov, and S. Harnett, "Chance-constrained optimal power flow: Risk-aware network control under uncertainty," *SIAM Review*, vol. 56, no. 3, pp. 461–495, 2014.
- [8] M. Lubin, Y. Dvorkin, and S. Backhaus, "A robust approach to chance constrained optimal power flow with renewable generation," *IEEE Trans. Power Syst.*, vol. 31, no. 5, pp. 3840–3849, 2016.
- [9] C. Ordoudis, V. A. Nguyen, D. Kuhn, and P. Pinson, "Energy and reserve dispatch with distributionally robust joint chance constraints," *Oper. Res. Lett.*, vol. 49, no. 3, pp. 291–299, 2021.
- [10] A. Shapiro, "Distributionally robust stochastic programming," *SIAM J. Optim.*, vol. 27, no. 4, pp. 2258–2275, 2017.
- [11] D. Kuhn, P. Mohajerin Esfahani, V. A. Nguyen, and S. Shafieezadeh-Abadeh, "Wasserstein distributionally robust optimization: Theory and applications in machine learning," *INFORMS Tut. Oper. Res. Manage. Sci. Age Anal.*, pp. 130–166, 2019.
- [12] J. M. Keynes, *A Treatise on Probability*. MacMillan & Co., 1921, London, UK.
- [13] E. Delage and Y. Ye, "Distributionally robust optimization under moment uncertainty with application to data-driven problems," *Oper. Res.*, vol. 58, no. 3, pp. 595–612, 2010.
- [14] W. Xie and S. Ahmed, "Distributionally robust chance constrained optimal power flow with renewables: A conic reformulation," *IEEE Trans. Power Syst.*, vol. 33, no. 2, pp. 1860–1867, 2018.
- [15] P. Mohajerin Esfahani and D. Kuhn, "Data-driven distributionally robust optimization using the Wasserstein metric: Performance guarantees and tractable reformulations," *Math. Prog.*, vol. 171, no. 1-2, pp. 115–166, 2017.
- [16] A. Arrigo, C. Ordoudis, J. Kazempour, Z. De Grève, J.-F. Toubeau, and F. Vallée, "Wasserstein distributionally robust chance-constrained optimization for energy and reserve dispatch: An exact and physically-bounded formulation," *Eur. J. Oper. Res.*, vol. 296, no. 1, pp. 304–322, 2022.
- [17] B. Li, R. Jiang, and J. L. Mathieu, "The value of including unimodality information in distributionally robust optimal power flow," 2018. [Online]. Available: <https://arxiv.org/abs/1811.10217>
- [18] A. Esteban-Pérez and J. M. Morales, "Partition-based distributionally robust optimization via optimal transport with order cone constraints," *4OR-Q. J. Oper. Res.*, 2021.
- [19] C. Wang, R. Gao, F. Qiu, J. Wang, and L. Xin, "Risk-based distributionally robust optimal power flow with dynamic line rating," *IEEE Trans. Power Syst.*, vol. 33, no. 6, pp. 6074–6086, 2018.
- [20] A. Arrigo, J. Kazempour, Z. D. Z., J.-F. Toubeau, and F. Vallée, "Enhanced Wasserstein distributionally robust OPF with dependence structure and support information," in *IEEE PowerTech 2021 Conference*, 2021, Madrid, Spain.
- [21] R. Gao and A. Kleywegt, "Data-driven robust optimization with known marginal distributions," 2017.
- [22] G. C. Pflug and M. Pohl, "A review on ambiguity in stochastic portfolio optimization," *Set-Valued Var. Anal.*, vol. 26, p. 733–757, 2018.
- [23] R. B. Neslen, *An Introduction to Copulas*. Springer, 1999, New York, USA.
- [24] A. Sklar, "Fonctions de répartition à n dimensions et leurs marges," *Publications de l'institut de statistiques de l'université de Paris*, vol. 8, pp. 229–231, 1959.
- [25] T. Ding, Q. Yang, X. Liu, C. Huang, Y. Yang, M. Wang, and F. Blaabjerg, "Duality-free decomposition based data-driven stochastic security-constrained unit commitment," *IEEE Trans. Sustain. Energy*, vol. 10, no. 1, pp. 82–93, 2019.
- [26] S. Agrawal, Y. Ding, A. Saberi, and Y. Ye, "Price of correlations in stochastic optimization," *Oper. Res.*, vol. 60, p. 150–162, 2012.
- [27] R. Gao and A. J. Kleywegt, "Distributionally robust stochastic optimization with dependence structure," 2017. [Online]. Available: <https://arxiv.org/abs/1701.04200>
- [28] F. Vallée, J. Lobry, and O. Deblecker, "Impact of the wind geographical correlation level for reliability studies," *IEEE Trans. Power Syst.*, vol. 22, no. 4, pp. 2232–2239, 2007.
- [29] Y. Guo, K. Baker, E. Dall'Anese, Z. Hu, and T. H. Summers, "Data-based distributionally robust stochastic optimal power flow – Part I: Methodologies," *IEEE Trans. Power Syst.*, vol. 34, no. 2, pp. 1483–1492, 2019.
- [30] A. Arrigo, J. Kazempour, Z. De Grève, J.-F. Toubeau, and F. Vallée, "Online companion: Embedding dependencies within distributionally robust optimization of modern power systems," 2021, available: <https://doi.org/10.5281/zenodo.5517996>.
- [31] H. Rahimian and S. Mehrotra, "Distributionally robust optimization: A review," 2019. [Online]. Available: <https://arxiv.org/abs/1908.05659>
- [32] D. Kuhn, W. Wiesemann, and A. Georghiou, "Primal and dual linear decision rules in stochastic and robust optimization," *Math. Prog.*, vol. 130, no. 1, pp. 177–209, 2011.
- [33] S. Zymler, D. Kuhn, and B. Rustem, "Distributionally robust joint chance constraints with second-order moment information," *Math. Prog.*, vol. 137, no. 1-2, pp. 167–198, 2013.
- [34] C. Ordoudis, P. Pinson, J. M. Morales, and M. Zugno, "An updated version of the IEEE RTS 24-bus system for electricity market and power system operation studies," 2016. [Online]. Available: <http://orbit.dtu.dk/files/120568114/An>
- [35] J. Kazempour and H. Zareipour, "Equilibria in an oligopolistic market with wind power production," *IEEE Trans. Power Syst.*, vol. 29, no. 2, pp. 686–297, 2014.
- [36] D. K. Molzahn, F. Dörfler, H. Sandberg, S. H. Low, S. Chakrabarti, R. Baldick, and J. Lavaei, "A survey of distributed optimization and control algorithms for electric power systems," *IEEE Trans. Smart Grid*, vol. 8, no. 6, pp. 2941–2962, 2017.